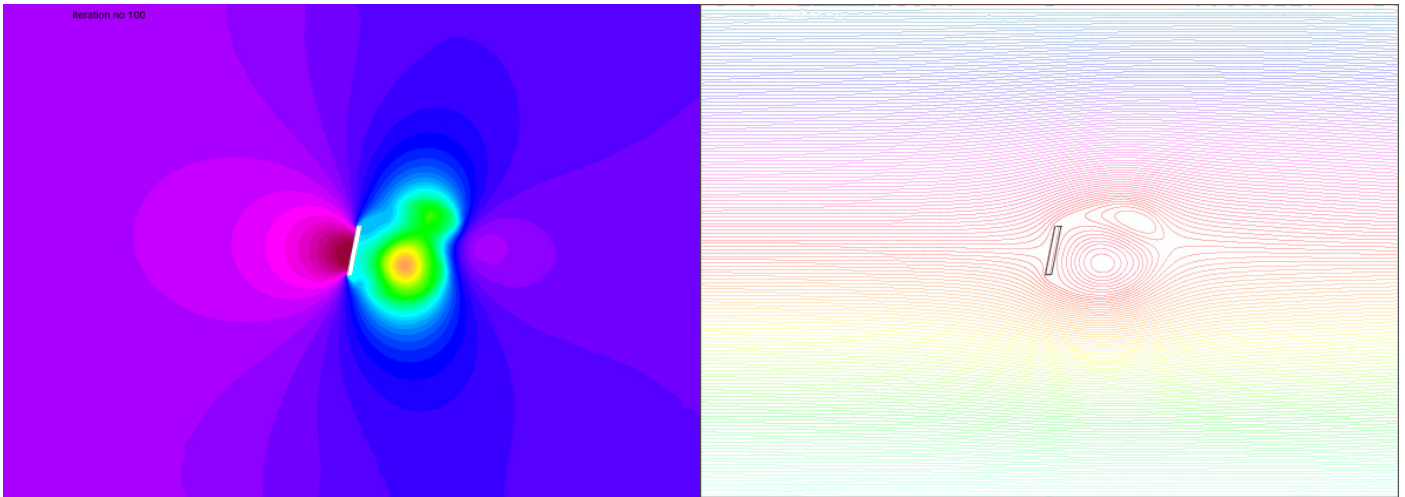


Figure 1: 2D simulation of the effects of a rectangular obstacle on a regular air stream at $t=100$ and with a ramp angle of 80%

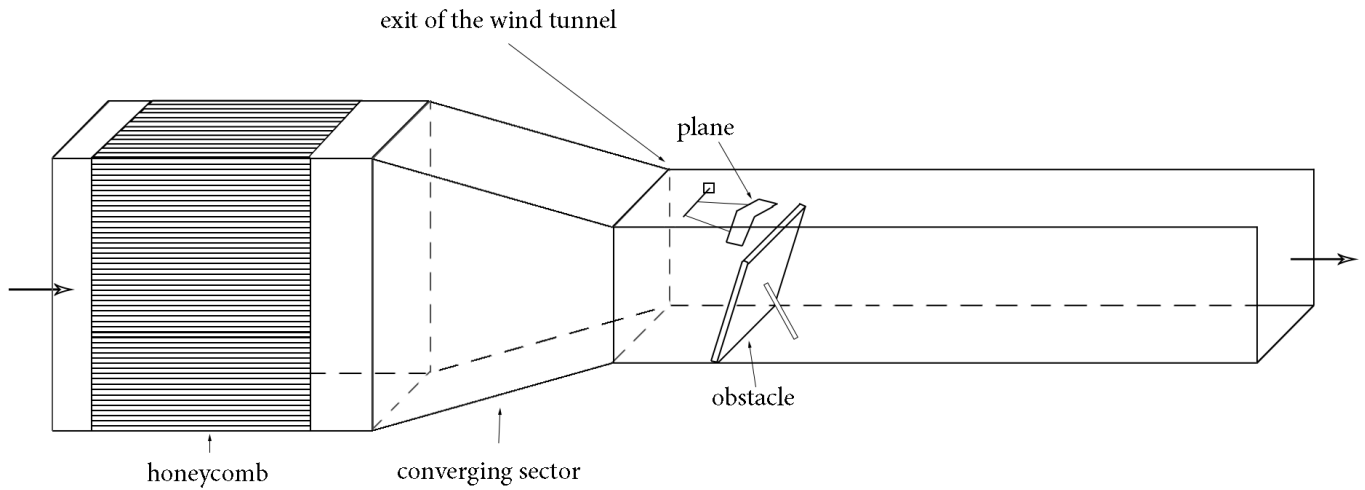


1a: Pressure field around the obstacle

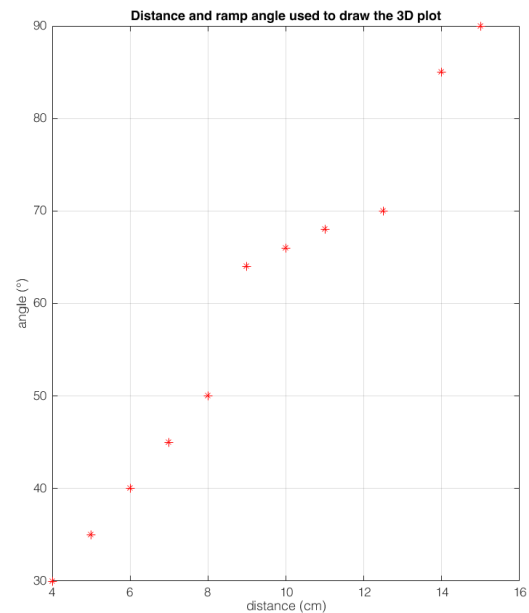
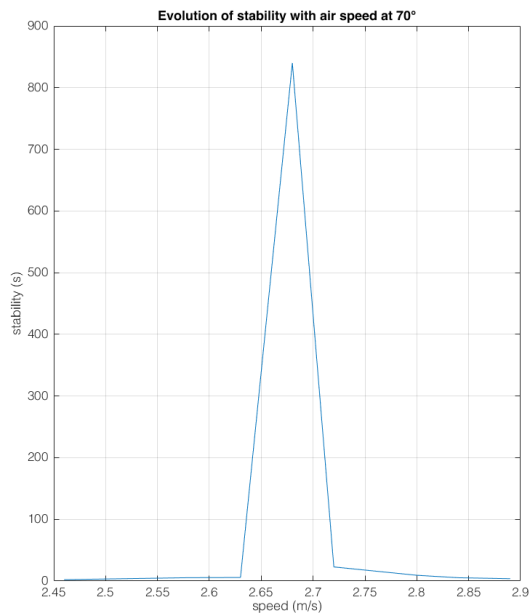
1b: Stream lines around the obstacle

Simulations conducted on FreeFem++ for a Reynolds of 10 000 which corresponds to the flight experiment ($L = 10^{-1}$ m; $V = 1$ m/s; in air). We applied ramp angles from 50% to 100% with a 10% increment. We also changed the thickness of the obstacle. These changes showed the impact of different parameters on our stream flow. Then we focused on our original experiment, which we simulated with a rectangular obstacle and a small ramp angle from the vertical. This gave us images of the pressure field and stream lines stabilizing our handglider.

Figure 2: Experimental set up for flight stability evaluation of a hand glider

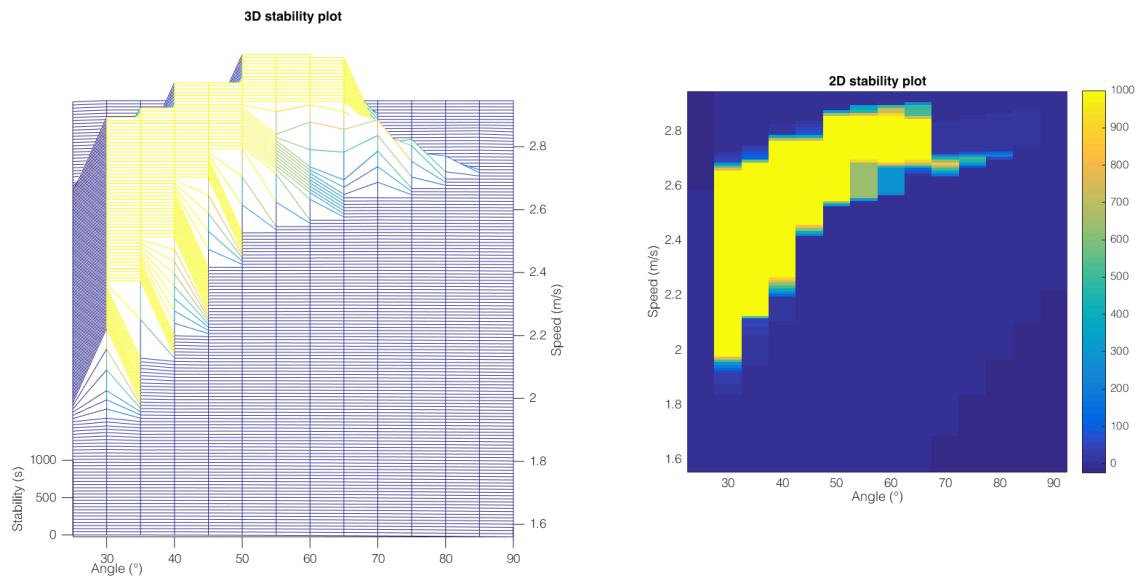


2a: Experimental set-up. We placed a rectangular plexiglass obstacle at the exit of the wind tunnel, which is open on top. We created a 3D printed glider similar to the foam one we used for the first gliding experiments. The plane is linked to an horizontal bar with two thin fishing line, in order to stop roll and pitch.



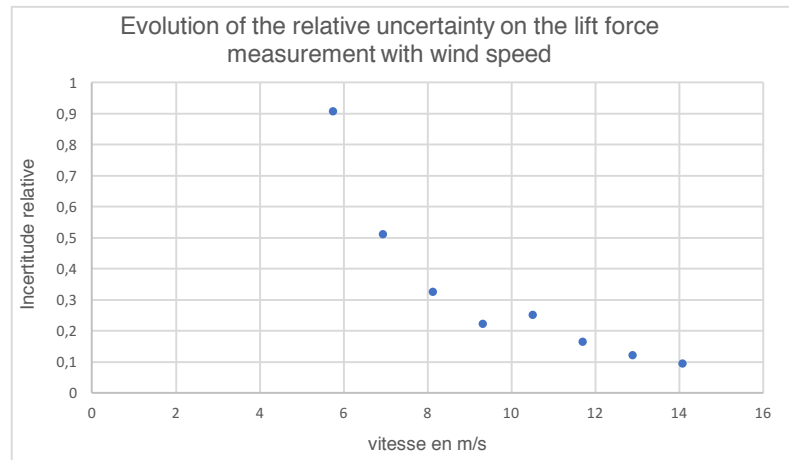
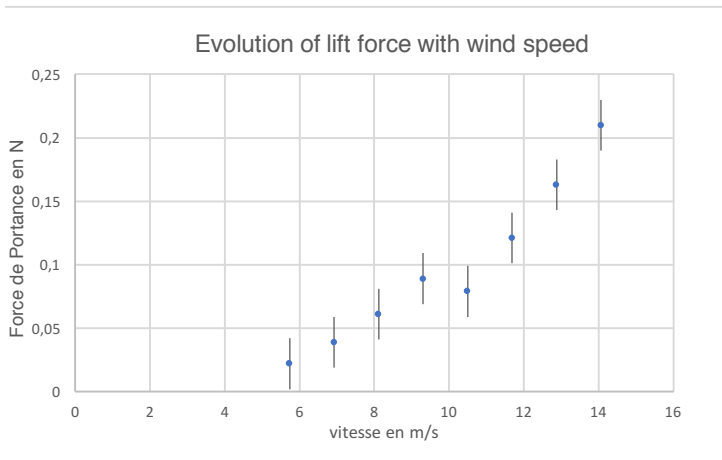
2b: Stability of the plane for 70° of ramp angle. We measured the variation of flight time with the speed of our laminar flow, in order to quantify its stability. This last parameter was changed with an incremental motor linked to the wind tunnel fan, and measured next to the horizontal bar with a hot-wire probe. When the glider had a stable flight (superior to 5 minutes), we decided to stop the measure and put it down as a 1000-second long flight. To have more precise mesures on the shorter flights, we did at least 10 flights, and took the average.

2c: Correspondance between ramp angle and distance to the exit of the tunnel of the obstacle. We measured the stability for different ramp angles and distances to the exit of the wind tunnel of the obstacle. The set-up needing a precise distance between the plane and the obstacle, we had to adjust the horizontal distance for each different angle. Since it required a certain amount of tests to find the right place, we took down all the positions in angle and distance and tried to follow a linear function.



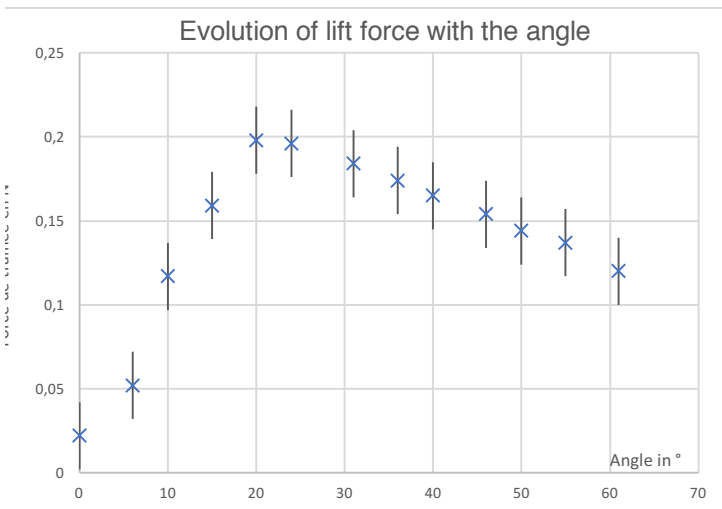
2d: Stability zone map in function of the ramp angle, the distance to the exit of the wind tunnel and the speed of flow.

Figure 3 : Study on the wind tunnel balance to determine the graph of drag coefficient and lift coefficient

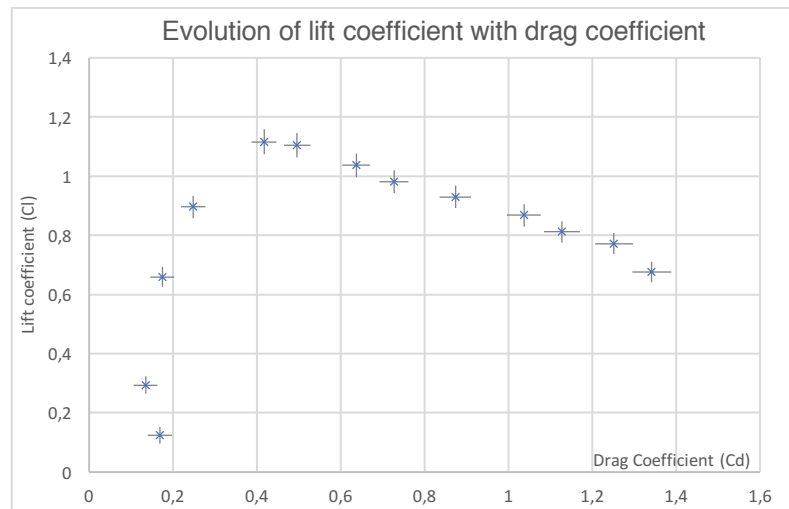


3a and 3b : determination of the wind speed of work

The figures show the diminution of the relative uncertainty on the lift force with the augmentation of the wind speed. The wind tunnel balance has a uncertainty of 0,02 N on the measured forces. Because the Reynolds number of our experiment stays in the same range between 1 and 14 m/s (over 1000 in any cases), it's relevant to work with a wind speed of 14 m/s event if the real experience occurs at a wind speed between 1 and 3 m/s.



3c: plot of evolution of the lift force with the angle at a wind speed of 14,06 m/s



3d: plot of the lift and drag coefficient

3c: The measurement is done by averaging the force applied to the aircraft during one minute. Before the measurement, a blank is done (measure with the support and without the aircraft) to provide more accurate results. The same type of graph is plot for the drag force evolution with the angle (not shown here).

3d: The lift and drag coefficient graph is obtained from the results of fig 3c, and we get the classic shape for the evolution of the lift coefficient. The maximum is for $C_d=0,41$ and $C_l=1,11$. Those values correspond to an angle of 20° which is consistent with the experiment.